Synthesis, Chemical Properties, and Biological Evaluation of CC-1065 and Duocarmycin Analogues Incorporating the 5-Methoxycarbonyl-1,2,9,9a-tetrahydrocyclopropa[*c*]benz[*e*]indol-4-one Alkylation Subunit

Dale L. Boger,* Terry V. Hughes, and Michael P. Hedrick

Department of Chemistry and The Skaggs Institute for Chemical Biology, The Scripps Research Institute, 10550 North Torrey Pines Road, La Jolla, California 92037

boger@scripps.edu

Received December 21, 2000

The synthesis of 5-methoxycarbonyl-1,2,9,9a-tetrahydrocyclopropa[*c*]benz[*e*]indol-4-one (C5-CO_2Me-CBI), a substituted CBI derivative bearing a C5 methoxycarbonyl group, and its corresponding 5-hydroxymethyl derivative are described in efforts to establish substituent electronic effects on the agents' functional reactivity and the resulting effect this has on their rate of DNA alkylation. Resolution of an immediate C5-CO_2Me-CBI precursor and its incorporation into both enantiomers of **16** and **17**, analogues of the duocarmycins, are also detailed. A study of the solvolysis reactivity and regioselectivity of *N*-BOC-C5-CO_2Me-CBI (**12**) revealed that the introduction of a C5 methyl ester modestly slowed the rate of solvolysis (1.8×, pH 3) without altering the inherent reaction regioselectivity (>20:1). The comparison of the X-ray structures of the *N*-CO_2Me derivatives of C5-CO_2Me-CBI and CBI revealed correlations with the reaction regioselectivity and the relative reactivity of the compounds. The latter correlated well with the less reactive C5-CO_2Me-CBI exhibiting a shortened N2−C2a bond length (1.386 vs 1.390 Å) and smaller χ_1 dihedral angle (8.1° vs 21.2°) indicative of greater vinylogous amide conjugation and was accompanied by a diminished (cross-conjugated) cyclopropane conjugation (shorter bond lengths). Establishment of the DNA alkyation properties revealed that C5-CO_2Me-CBI-based agents retained the identical alkylation selectivity of the natural products. More importantly, the C5 methyl ester was found to decrease the rate (0.77×) of DNA alkylation relative to CBI, consistent with its inherent lower reactivity. These results indicate that the previously observed increase in the rate of DNA alkylation for C7-substituted CBI analogues including CCBI (7-cyano-CBI) is contrary to expectations based on their inherent reactivities. Unlike **17**, in which the C5 methyl ester does not bind in the minor groove, the C7 substituent lies in the minor groove extending the rigid length of the agents, further enhancing the DNA binding-induced conformational change responsible for activation toward nucleophilic attack and catalysis of the DNA alkylation reaction.

(+)-CC-1065 (**1**) and the duocarmycins (**2** and **3**) are the primary members of a class of potent antitumor antibiotics that derive their biological effects through the reversible, sequence-selective alkylation of duplex DNA, Figure 1.[1−3]

In previous studies, we detailed the synthesis and evaluation of natural product analogues containing the 1,2,9,9a-tetrahydrocyclopropa[*c*]benz[*e*]indol-4-one (CBI) alkylation subunit.[4,5] Significantly, the natural enantiomers of the CBI-based analogues of CC-1065 and the duocarmycins have proven chemically more stable (4×), biologically more potent (4×), and synthetically more accessible than the corresponding agents incorporating the natural alkylation subunit of CC-1065. In addition, we previously probed the importance of substitution at the C7 position of CBI-based analogues.[6,7] These studies entailed the preparation and evaluation of 7-methoxy-1,2,9,9a-tetrahydrocylopropa[*c*]benz[*e*]indol-4-one (MCBI)[6] bearing a C7 methoxy substituent and 7-cyano-1,2,9,9a-tetrahydrocyclopropa[*c*]benz[*e*]indol-4-one (CCBI)[7] bearing a C7 cyano group. The side-by-side evaluation of a set of agents containing the CBI, MCBI, and CCBI alkylation subunits allowed an assessment of the effects of a C7 substituent on their chemical and functional reactivity as well as their biological properties

(1) Boger, D. L.; Johnson, D. S. *Angew. Chem., Int. Ed. Engl.* **1996**, *35*, 1439. Boger, D. L.; Johnson, D. S. *Proc. Natl. Acad. Sci. U.S.A.* **1995**, *92*, 3642.

(2) Boger, D. L. *Chemtracts: Org. Chem.* **1991**, *4*, 329.

(3) Warpehoski, M. A.; Hurley, L. H. *Chem. Res. Toxicol.* **1988**, *1*, 315. Hurley, L. H.; Needham-VanDevanter, D. R. *Acc. Chem. Res.* **1986**, *19*, 230.

(4) Boger, D. L.; Ishizaki, T.; Wysocki, R. J., Jr.; Munk, S. A.; Kitos, P. A.; Suntornwat, O. *J. Am. Chem. Soc.* **1989**, *111*, 6461. Boger, D. L.; Ishizaki, T.; Kitos, P. A.; Suntornwat, O. *J. Org. Chem.* **1990**, *55*, 5823.

(5) Boger, D. L.; Ishizaki, T.; Zarrinmayeh, H.; Kitos, P. A.; Suntornwat, O. *Bioorg. Med. Chem. Lett.* **1991**, *1*, 55. Boger, D. L.; Ishizaki, T.; Sakya, S. M.; Munk, S. A.; Kitos, P. A.; Jin, Q.; Besterman, J. M. *Bioorg. Med. Chem. Lett.* **1991**, *1*, 115. Boger, D. L.; Munk, S. A. *J. Am. Chem. Soc.* **1992**, *114*, 5487. Boger, D. L.; Yun, W.; Teegarden, B. R. *J. Org. Chem.* **1992**, *57*, 2873. Boger, D. L.; Yun, W. *J. Am. Chem. Soc.* **1994**, *116*, 7996. Boger, D. L.; McKie, J. A. *J. Org. Chem.* **1995**, *60*, 1271. Boger, D. L.; Yun, W.; Cai, H.; Han, N. *Bioorg. Med. Chem.* **1995**, *3*, 761. Boger, D. L.; Yun, W.; Han, N. *Bioorg. Med. Chem.* **1995**, *3*, 1429. Boger, D. L.; McKie, J. A.; Boyce, C. W. *Synlett* **1997**, 515. Boger, D. L.; Boyce, C. W.; Garbaccio, R. M.; Searcey, M.; Jin, Q. *Synthesis* **1999**, 1505.

(6) Boger, D. L.; McKie, J. A.; Cai, H.; Cacciari, B.; Baraldi, P. G. *J. Org. Chem.* **1996**, *61*, 1710.

(7) Boger, D. L.; Han, N.; Tarby, C. M.; Boyce, C. W.; Cai, H.; Jin, Q.; Kitos, P. A. *J. Org. Chem.* **1996**, *61*, 4894.

10.1021/jo001772g CCC: $20.00
Published on Web 03/13/2001

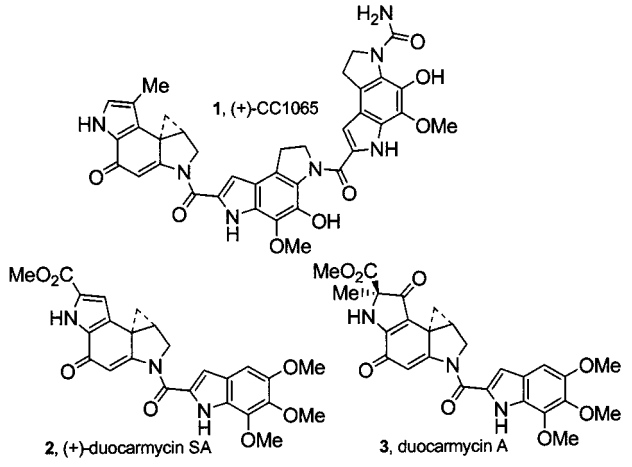

Figure 1.

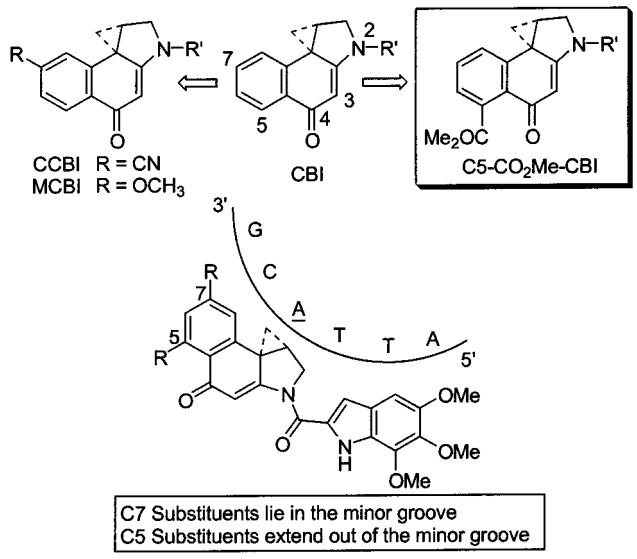

Figure 2.

(Figure 2). Studies of MCBI revealed a modest increase (1.2−1.06×) in the rate of acid-catalyzed solvolysis compared to that of CBI, and the corresponding studies of CCBI showed a small decrease (0.68−0.51×) in the rate of solvolysis. Although these trends were expected, the magnitude of the effect was small and a classical Hammett quantitation indicated a very small C7 substituent influence on functional reactivity ($\rho = -0.3$). With this in mind, it was unexpected to observe that the rates of DNA alkylation for both MCBI and CCBI were faster than that of CBI, which indicated that substituent effects beyond their electronic effects on intrinsic reactivity were contributing to the properties. These results proved consistent with observations made in examining the role of the duocarmycin SA C6 methyl ester, which was found to enhance chemical stability (6×) but accelerate the rate (12−13×) and efficiency (10×) of DNA alkylation.[8] While these substituent effects on the DNA alkylation rate are unexpected on the basis of their effect on intrinsic reactivity, they are consistent with a role in which they serve to extend the rigid length of the alkylation subunit, resulting in an increase in the DNA binding-induced conformational change that serves to deconjugate the vinylogous amide and activate the alkylation subunit for nucleophilic attack.[9−18]

In efforts to further define substituent effects of substituted CBI analogues, herein we report the preparation and evaluation of 5-methoxycarbonyl-1,2,9,9a-tetrahydrocyclopropa[*c*]benz[*e*]indol-4-one (C5-CO_2Me-CBI), bearing a C5 methyl ester that cannot lie in the minor groove upon complex formation with DNA. The comparison of analogues incorporating this modified alkylation subunit with the previously described CBI analogues was anticipated to clarify the substituent roles and establish more clearly the electronic effects of a substituent on the chemical reactivity and biological properties of the agents.

Synthesis of C5-CO_2Me-CBI (13) and *N*-BOC-C5-CO_2Me-CBI (12).[19] The conversion of 3-nitronaphthostyril (**4**)[20] to 3-nitro-1,8-naphtholactone (**5**)[21] was effected by a three-step sequence of hydrolysis (0.5 N NaOH, reflux, 1 h), diazotization ($NaNO_2$, 1 N H_2SO_4, 0 °C), and thermally induced decomposition of the diazonium salt with concomitant intramolecular cyclization (0−85 °C). Subsequent methanolysis (H_2SO_4, CH_3OH, 100%) of the lactone provided **6** (Scheme 1). Reduction of the nitro group of **6** (H_2, 10% Pd/C, THF, 2 h) followed by BOC protection of the naphthylamine (BOC_2O, THF, reflux, 9 h) afforded **7** (two steps, 87% overall). Protection of the phenol as a MOM ether to provide **8** (MOMCl, CH_2Cl_2, *i*-Pr_2NEt, 92%) and low-temperature, acid-catalyzed C4 bromination (NBS, TsOH, THF, −78 °C, 1 h, 91%) provided **9**. Alkylation of the sodium salt of **9** (NaH, DMF, 0−25 °C, 30 min) with 1,3-dichloropropene (25 °C, 12 h, 91%) provided **10**, the key substrate for free radical cyclization,[22] as a mixture of *E*/*Z* isomers. The 5-*exo*-*trig* free radical cyclization occurred smoothly in benzene (80 °C, 0.1 equiv of AIBN, 1.1 equiv of Bu_3SnH, 2 h, 95%) to

(8) Boger, D. L.; Santillán, A., Jr.; Searcey, M.; Brunette, S. R.; Wolkenberg, S. E.; Hedrick, M. P.; Jin, Q. *J. Org. Chem.* **2000**, *65*, 4101.

(9) Boger, D. L.; Garbaccio, R. M. *Acc. Chem. Res.* **1999**, *32*, 1043. Boger, D. L.; Garbaccio, R. M. *Bioorg. Med. Chem.* **1997**, *5*, 263.

(10) Boger, D. L.; Bollinger, B.; Hertzog, D. L.; Johnson, D. S.; Cai, H.; Mésini, P.; Garbaccio, R. M.; Jin, Q.; Kitos, P. A. *J. Am. Chem. Soc.* **1997**, *119*, 4987.

(11) Eis, P. G.; Smith, J. A.; Rydzewski, J. M.; Case, D. A.; Boger, D. L.; Chazin, W. J. *J. Mol. Biol.* **1997**, *272*, 237. Schnell, J. R.; Ketchem, R. R.; Boger, D. L.; Chazin, W. J. *J. Am. Chem. Soc.* **1999**, *121*, 5645. Smith, J. A.; Bifulco, G.; Case, D. A.; Boger, D. L.; Gomes-Paloma, L.; Chazin, W. J. *J. Mol. Biol.* **2000**, *300*, 1195.

(12) Boger, D. L.; Hertzog, D. L.; Bollinger, B.; Johnson, D. S.; Cai, H.; Goldberg, J.; Turnbull, P. *J. Am. Chem. Soc.* **1997**, *119*, 4977.

(13) Boger, D. L.; Garbaccio, R. M.; Jin, Q. *J. Am. Chem. Soc.* **1997**, *62*, 88875.

(14) Boger, D. L.; Santillán, A., Jr.; Searcey, M.; Jin, Q. *J. Am. Chem. Soc.* **1998**, *120*, 11554.

(15) Boger, D. L.; Santillán, A., Jr.; Searcey, M.; Jin, Q. *J. Org. Chem.* **1999**, *64*, 5241.

(16) Boger, D. L.; Turnbull, P. *J. Org. Chem.* **1997**, *62*, 5849.

(17) Boger, D. L.; Turnbull, P. *J. Org. Chem.* **1998**, *63*, 8004.

(18) Boger, D. L.; Garbaccio, R. M. *J. Org. Chem.* **1999**, *64*, 5666.

(19) For a review of synthetic approaches to CC-1065 and the duocarmycins and their analogues, see: Boger, D. L.; Boyce, C. W.; Garbaccio, R. M.; Goldberg, J. *Chem. Rev.* **1997**, *97*, 787.

(20) Plakidin, V. L.; Vostrova, V. N.; Gnatyuk, P. P.; Zadorozhnyi, N. M. *Zh. Org. Khim.* **1977**, *13*, 2194. Plakidin, V. L.; Zadorozhnyi, N. M.; Krasota, Z. I. *Zh. Org. Khim.* **1970**, *6*, 1480.

(21) Lactone **5** was prepared following a procedure previously disclosed: Birch, A. J.; Salahud-Din, M.; Smith, D. C. C. *J. Chem. Soc. C* **1966**, 523. For **5**: yellow solid, mp 193−195 °C; ^{1}H NMR (acetone-d_6, 250 MHz) δ 8.92 (d, J = 1.4 Hz, 1H), 8.69 (d, J = 8.3 Hz, 1H), 8.48 (d, J = 7.4 Hz, 1H), 8.18 (apparent t, J = 7.8 Hz, 1H), 8.01 (d, J = 1.4 Hz, 1H); IR (film) ν_{max} 3097, 1815, 1785, 1538 cm^{-1}; EIMS *m*/*z* 215 (M^+).

(22) Patel, V. F.; Andis, S. L.; Enkema, J. K.; Johnson, D. A.; Kennedy, J. H.; Mohamadi, F.; Schultz, R. M.; Soose, D. J.; Spees, M. M. *J. Org. Chem.* **1997**, *62*, 8868. Boger, D. L.; Boyce, C. W.; Garbaccio, R. M.; Searcey, M. *Tetrahedron Lett.* **1998**, *39*, 2227.

Scheme 1

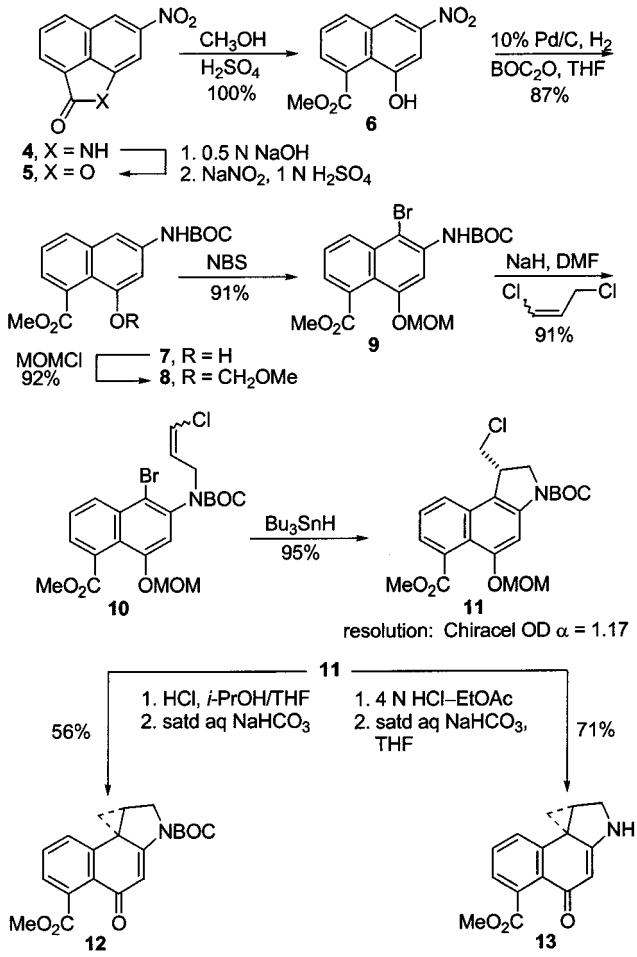

afford **11**, the MOM protected precursor to *N*-BOC-C5-CO_2Me-CBI. Removal of the MOM ether of **11** (HCl, *i*-PrOH/THF) followed by treatment with saturated aqueous $NaHCO_3$ induced spirocyclization and afforded **12** (56%). Similarly, acid-catalyzed global deprotection of **11** (4 N HCl/EtOAc, 25 °C, 45 min) followed by spirocyclization of the crude indoline hydrochloride salt **14** upon exposure to 5% aqueous $NaHCO_3$−THF (1:1, 25 °C, 2 h, 71%) cleanly provided **13**.

Resolution. The advanced intermediate **11** was resolved directly on a semipreparative Daicel Chiracel OD column ($\alpha = 1.17$).[23] For our purposes, sufficient quantities of **11** could be separated on a semipreparative 10 μm, 2 cm × 25 cm HPLC OD column (2% *i*-PrOH/hexane, 14 mL/min) with a 90−100% recovery of the total sample and routinely provided the two enantiomers of **11** in greater than 99% ee. Subjection of both enantiomers of **11** to the deprotection and subsequent spirocyclization provided the enantiomers of **12** and **13**. The assignment of the absolute configuration was tentatively based upon the optical rotations of **12** and **13** for which a strong positive rotation was assigned the natural configuration, which agrees with previous studies, and was further established in the subsequent biological studies. In particular, the distinct DNA alkylation selectivities characteristic of the natural and unnatural enantiomers were found to be in agreement with these initial assignments.

C5-CO_2Me-CBI-TMI (17). The C5-CO_2Me-CBI alkylation subunit was incorporated into the duocarmycin

(23) Boger, D. L.; Yun, W. *J. Am. Chem. Soc.* **1994**, *116*, 7996.

Scheme 2

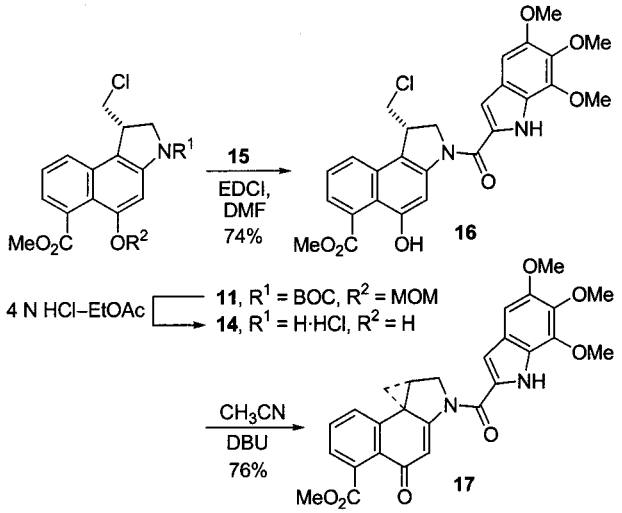

Table 1. Acid-Catalyzed Solvolysis Reactivity

	N-BOC-MCBI	*N*-BOC-CBI	*N*-BOC-CCBI	**12**
k, s^{-1} (pH 3.0)	1.75×10^{-6}	1.45×10^{-6}	0.99×10^{-6}	0.81×10^{-6}
$t_{1/2}$, h (pH 3.0)	110	133	213	236
k, s^{-1} (pH 2.0)	1.62×10^{-5}	1.53×10^{-5}	0.78×10^{-5}	0.79×10^{-5}
$t_{1/2}$, h (pH 2.0)	11.8	12.5	24.2	24.7

analogues **16** and **17** as detailed in Scheme 2. Acid-catalyzed deprotection of **11** (4 N HCl/EtOAc, 25 °C, 30 min, quantitative) followed by coupling of the unstable indoline hydrochloride salt **14** with 5,6,7-trimethoxyindole-2-carboxylic acid (**15**, 3 equiv of EDCI, DMF, 25 °C, 12 h, 74%) conducted in the deliberate absence of base provided **16**. Subsequent treatment of **16** with DBU (2 equiv, 25 °C, 1 h) provided **17** (76%). Notably, the use of the MOM versus more common benzyl ether protecting group for the phenol permitted a single step versus two step conversion of **11** to **14**.

Chemical Solvolysis: Reactivity. The first property of the agents that was studied was their relative reactivity toward solvolysis, which reflects their relative functional reactivity for acid-catalyzed nucleophilic addition.[1] Our previous study of CCBI revealed that the introduction of the strong electron-withdrawing C7 cyano group modestly slowed acid-catalyzed solvolysis (0.68−0.51×).[7] As expected, acid-catalyzed solvolysis of **12** ($k = 0.81 \times 10^{-6}$ s^{-1}, $t_{1/2} = 236$ h, pH 3.0 and $k = 0.78 \times 10^{-5}$ s^{-1}, $t_{1/2} = 24.7$ h, pH 2.0) did occur more slowly than *N*-BOC-CBI ($k = 1.45 \times 10^{-6}$ s^{-1}, $t_{1/2} = 133$ h, pH 3.0)[4] and at a rate comparable to *N*-BOC-CCBI ($k = 0.99 \times 10^{-6}$ s^{-1}, $t_{1/2} = 213$ h, pH 3.0)[7] (Table 1).

The solvolysis was conducted in a 1:1 CH_3OH/buffer (pH 3.0; buffer = 4:1:20 v:v:v 0.1 M citric acid, 0.2 M Na_2HPO_4, H_2O) and was monitored spectrophotometrically by UV with the disappearance of a long-wavelength absorption of **12** (313 nm) and with the appearance of a short-wavelength absorption (260 nm) corresponding to the solvolysis products (Figure 3).[24]

Chemical Solvolysis: Regioselectivity. Treatment of **12** with 0.12 equiv of CF_3SO_3H in CH_3OH (0 °C, 72 h)

(24) Differing from past observations, the *N*-BOC group of *N*-BOC-C5-CO_2Me-CBI (**12**) was found to hydrolyze slowly at pH 7 ($t_{1/2} > 1000$ h; 40 days) whereas *N*-BOC-CBI is stable to both hydrolysis and solvolysis at pH 7.

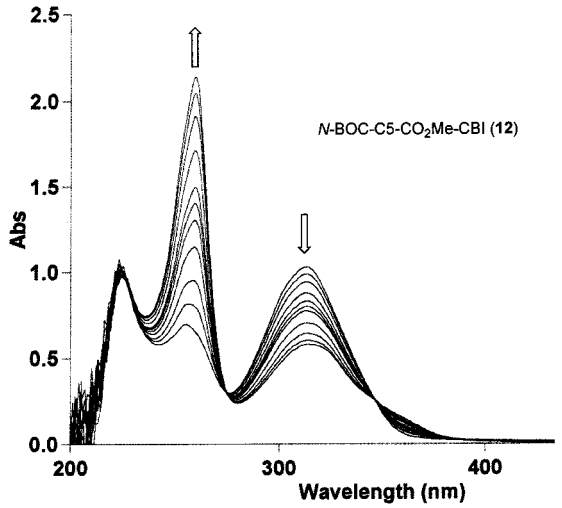

Figure 3. UV spectra of solvolysis study of **12** at pH 3.0 conducted in 50% CH_3OH/buffer (4:1:20 v:v:v 0.1 M citric acid, 0.2 M $NaHPO_4$, H_2O). The spectra shown were recorded at 0, 30, 71, 119, 167, 198, 240, 334, 440, 542, and 648 h.

Scheme 3

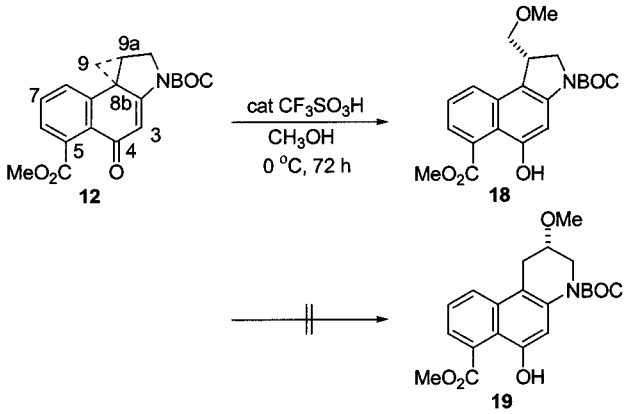

resulted in the clean solvolysis to provide a single product **18** (75%, 92% based on recovered **12**, Scheme 3). Clean cleavage of the C8b−C9 bond with addition of CH_3OH to the least substituted C9 cyclopropane carbon to provide **18** was observed, and no ring expansion solvolysis with cleavage of the C8b−C9a bond to provide **19** was detected (>20:1) even in the crude ^1H NMR of the solvolysis reaction mixture. This is consistent with prior studies of *N*-BOC-CBI and related alkylation subunits (CCBI, MCBI) where no (>20:1) ring expansion solvolysis product was detected[4−7] but is distinct from the behavior of the natural product alkylation subunits where substantial (**3**, 3:2) or significant (**1**, 4:1; **2**, 6:1) ring expansion is observed.[25,26]

X-ray Structure of 21: Correlation with Reactivity and Reaction Regioselectivity. Although the *N*-BOC derivative **12** did not provide crystals suitable for X-ray analysis, the corresponding *N*-CO_2Me derivative **21** was prepared (Scheme 4) and provided X-ray quality white plates upon crystallization from EtOAc/hexane.

The structural details of **21** and their comparison with those of *N*-CO_2Me-CBI highlight several important re-

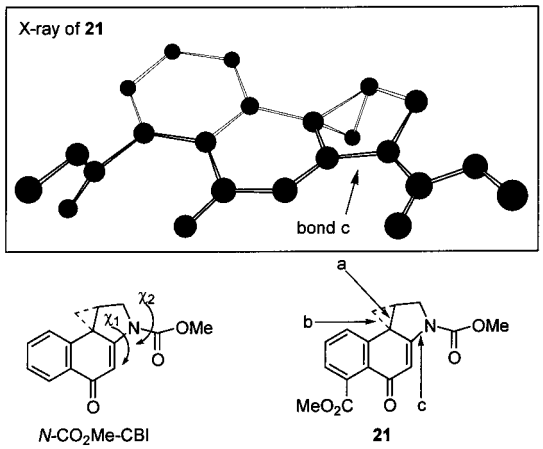

X-ray bond length, Å	*N*-CO_2Me-CBI	**21**
a	1.521	1.514
b	1.544	1.538
c	1.390 ± 0.005	1.386 ± 0.0017
X-ray dihedral angles		
χ_1	21.2°	8.1°
χ_2	4.5°	4.0°
Solvolysis reactivity		
$t_{1/2}$ (pH 3)	133 h	236 h

Figure 4.

Scheme 4

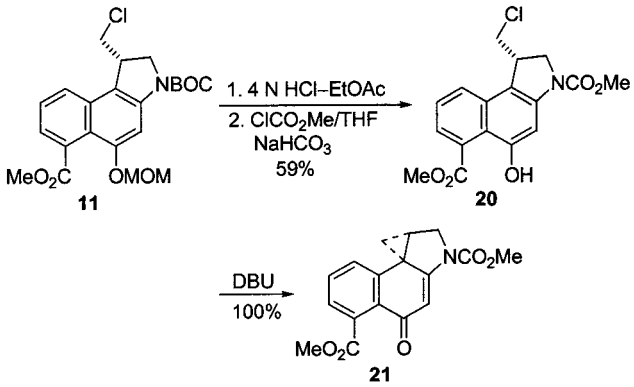

lationships between the structure, reactivity, and reaction regioselectivity. First, the structure of **21** reinforces important insights into the solvolysis regioselectivity that have been derived from the prior structural studies in the series.[6,7,12,26] The distinguishing feature controlling the regioselectivity appears to be the relative stereoelectronic alignment[27,28] of the two cyclopropane bonds available for cleavage and **21** conforms to this beautifully (Figure 4).

The C8b−C9 bond and its bent orbitals are nearly perpendicular to the plane of the cyclohexadienone and aligned to become a part of the solvolysis product phenol π-system, whereas the C8b−C9a bond nearly lies in the plane of the cyclohexadienone orthogonal to the π-system. This alignment of the C8b−C9 bond by **21** is at least as good or better than that of *N*-CO_2Me-CBI itself. Consistent with this conjugation with the π-system, the reactive C8b−C9 bond (1.538 Å) is longer than the

(25) Warpehoski, M. A.; Harper, D. E. *J. Am. Chem. Soc.* **1994**, *116*, 7573. Warpehoski, M. A.; Harper, D. E. *J. Am. Chem. Soc.* **1995**, *117*, 2951.

(26) Boger, D. L.; Goldberg, J.; McKie, J. A. *Bioorg. Med. Chem. Lett.* **1996**, *6*, 1955. Boger, D. L.; McKie, J. A.; Nishi, T.; Ogiku, T. *J. Am. Chem. Soc.* **1997**, *119*, 311.

(27) Boger, D. L.; Mésini, P.; Tarby, C. M. *J. Am. Chem. Soc.* **1994**, *116*, 6461. Boger, D. L.; Mésini, P. *J. Am. Chem. Soc.* **1994**, *116*, 11335. Boger, D. L.; Mésini, P. *J. Am. Chem. Soc.* **1995**, *60*, 1271.

(28) Boger, D. L.; Jenkins, T. J. *J. Am. Chem. Soc.* **1996**, *118*, 8860.

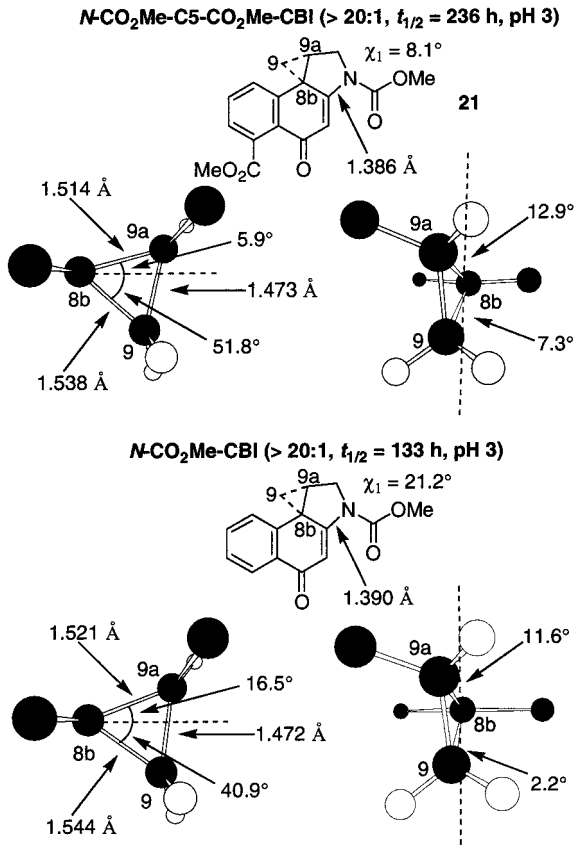

Figure 5. Stick models of the side view and 90° rotation view of the activated cyclopropane of **21** and *N*-CO_2Me-CBI illustrating data taken from the X-ray crystal structures and highlighting the stereoelectronic alignment of the cyclopropane with the cyclohexadienone π-system.

unreactive C8b−C9a bond (1.514 Å). Thus, only the observed cleavage of the C8b−C9 bond with nucleophilic attack on C9 would be expected (Figure 5).

Prior structural studies in the series have also shown correlations between pH 3 reactivity and the N2−C2a bond length diagnostic of the extent of vinylogous amide conjugation.[9,16] Consistent with the relative reactivity of **12** versus *N*-BOC-CBI, the N2−C2a bond length is slightly shorter within **21** versus *N*-CO_2Me-CBI (1.386 vs 1.390 Å) indicating a slightly higher degree of vinylogous amide conjugation which is reflected in its greater stability. Tracking with this greater stability, the extent of vinylogous amide conjugation, and the N2−C2a bond length, are the observed χ_1 and χ_2 dihedral angles.[16] The X-ray of **21** indicates a smaller χ_1 dihedral angle (8.1° vs 21.2°) and a comparable χ_2 dihedral angle (4.0° vs 4.5°), which is consistent with its enhanced vinylogous amide conjugation (Figure 6).

Even more beautifully, the composite bond lengths of the cyclopropane are longer with *N*-CO_2Me-CBI than with **21**. Both the C8b−C9 bond length of **21** versus *N*-CO_2Me-CBI (1.538 vs 1.544 Å) and the C8b−C9a bond length (1.514 vs 1.521 Å) are shorter indicative of the greater stability and diminished conjugation. Thus, the greater cross-conjugated vinylogous amide stabilization of **21** versus *N*-CO_2Me-CBI (N2−C2a bond length of 1.386 vs 1.390 Å) diminishes the relative extent of the cyclopropane conjugation, and this is reflected in its relative cyclopropane bond lengths and its reactivity (Figures 4 and 5). An additional subtle ramification of this diminished cyclopropane conjugation of **21** is the slightly less effective backside alignment of the reactive C8b−C9 bond (7.3° vs 2.2°, Figure 5).[16]

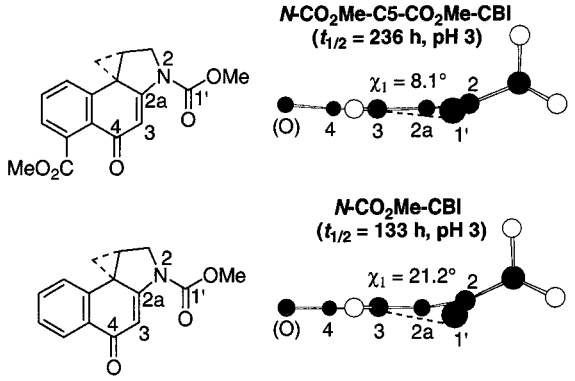

Figure 6. Stick models of the vinylogous amide profile for **21** and *N*-CO_2Me-CBI illustrating data taken from X-ray crystal structures and highlighting the χ_1 dihedral angle of the vinylogous amide.

Finally and interestingly, the ester adopts a twisted arrangement relative to the plane of the aromatic ring, minimizing a destabilizing electrostatic lone pair/lone pair interaction between the C4 carbonyl and the ester oxygens that would be present in either planar orientation.

DNA Alkylation Selectivity and Efficiency. The DNA alkylation properties of the agents were examined within duplex w794 DNA,[29] which allowed for comparison with the results available for related agents. The alkylation site identification and the assessment of the relative selectivity among the available sites were obtained by thermally induced strand cleavage of the singly 5′ end-labeled duplex DNA after exposure to the agents. After treatment of the end-labeled duplex DNA with a range of agent concentrations, the unbound agent was removed by EtOH precipitation of the DNA. Redissolution of the DNA in aqueous buffer, thermolysis (100 °C, 30 min) to induce depurination at the sites of DNA alkylation, denaturing high-resolution polyacrylamide gel electrophoresis (PAGE) adjacent to Sanger dideoxynucleotide sequencing standards, and autoradiography led to identification of the DNA cleavage and alkylation sites. The complete details of this procedure have been disclosed elsewhere.[29] The natural enantiomers of **17** and its seco precursor **16** were found to alkylate DNA in an indistinguishable fashion and with selectivities and efficiencies identical to (+)-duocarmycin SA (**2**) and (+)-CBI-TMI (Figure 7), where **16** and **17** detectably alkylate the same high affinity site of 5′-AATTA at 10^{-5}−10^{-6} M (25 °C, 24 h).

Similarly, the unnatural enantiomers of **16** and **17** behaved indistinguishably and alkylated DNA with the same selectivity as *ent*-(−)-duocarmycin SA and *ent*-(−)-CBI-TMI (data not shown).[23,30] Characteristic of such unnatural enantiomers, the alkylation reaction was much slower and less efficient (100×) than the corresponding natural enantiomer. Thus, alkylation of w794 DNA was observed at 10^{-4} versus 10^{-6} M and even then required more vigorous conditions (37 vs 25 °C) and longer

(29) Boger, D. L.; Munk, S. A.; Zarrinmayeh, H.; Ishizaki, T.; Haught, J.; Bina, M. *Tetrahedron* **1991**, *47*, 2661.
(30) Boger, D. L.; Johnson, D. S.; Yun, W. *J. Am. Chem. Soc.* **1994**, *116*, 1635.

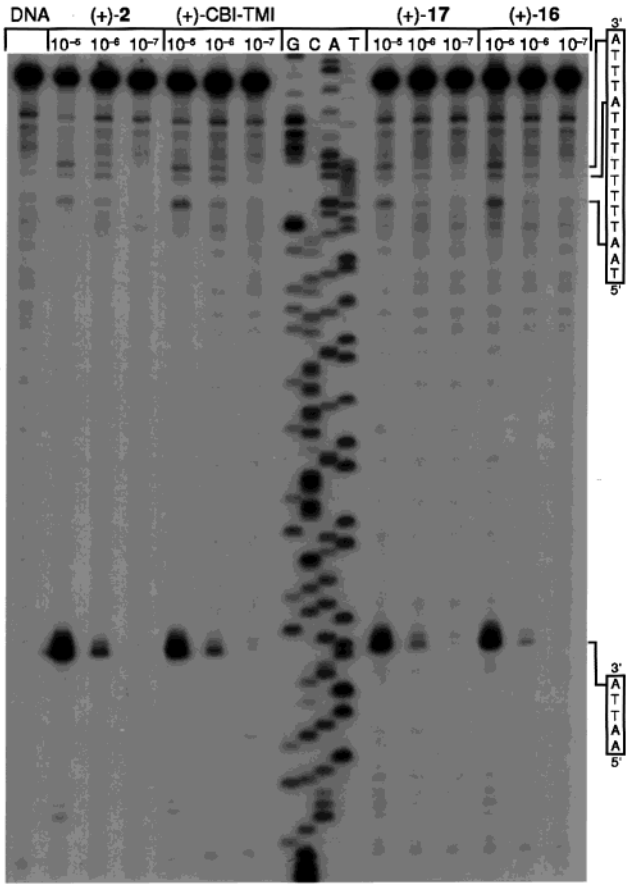

Figure 7. Thermally induced strand cleavage of double-stranded DNA (SV40 DNA fragment, 144 bp, nucleotide no. 5238−138, clone w794) after 24 h incubation of agent-DNA at 25 °C followed by removal of unbound agent and 30 min incubation at 100 °C; denaturing PAGE and autoradiography. Lane 1, control DNA; lanes 2−4, (+)-duocarmycin SA (**2**, 1×10^{-5} to 1×10^{-7} M); lanes 5−7, (+)-CBI-TMI (1×10^{-5} to 1×10^{-7} M); lanes 8−11, Sanger G, C, A, and T reactions; lanes 12−14, (+)-**17** (1×10^{-5} to 1×10^{-7} M); lanes 15−17, natural enantiomer of **16** (1×10^{-5} to 1×10^{-7} M).

reaction times (48−72 vs 24 h). Unlike the natural enantiomers where **16**, **17**, (+)-duocarmycin SA, and (+)-CBI-TMI exhibited near equivalent efficiencies (25 °C, 24 h, Figure 7), *ent*-(−)-**17** was even slower (72 h, 37 °C) at alkylating DNA than *ent*-(−)-CBI-TMI, but like *ent*-(−)-CBI-TMI, it was approximately 10× less efficient at alkylating DNA than *ent*-(−)-duocarmycin SA (24 h, 37 °C).

Rate of DNA Alkylation. Analogous to prior studies, the relative rate of DNA alkylation for (+)-**17** versus that of (+)-CBI-TMI, for which comparisons have been made with (+)-MCBI-TMI and (+)-CCBI-TMI, was measured at the single high affinity 5′-AATTA site in w794 DNA. In prior studies, the relative rates of DNA alkylation for MCBI-TMI (1.9×), CBI-TMI (1×), and CCBI (2.5×) were established and revealed that an agent substituted at the C7 position displayed an increased rate of DNA alkylation regardless of whether the substituent was electron-donating (MCBI) or electron-withdrawing (CCBI).[6,7]

The current study revealed that the relative rate of DNA alkylation for (+)-**17** versus (+)-CBI-TMI was 0.77× (Figure 8). Thus, the intrinsic reduced reactivity of (+)-**17** relative to (+)-CBI-TMI directly correlates with its reduced rate of DNA alkylation. This result underscores the unique behavior of (+)-CCBI-TMI which alkylates

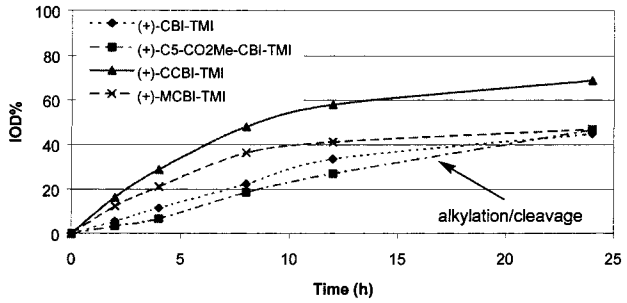

Figure 8. Plot of percent integrated optical density (IOD%) versus time established through autoradiography of 5′-^{32}P end-labeled DNA and used to monitor the relative rate of w794 alkylation at the 5′-AATTA high affinity site for (+)-C5-CO_2MeCBI-TMI (**17**), (+)-CBI-TMI, (+)-CCBI-TMI, and (+)-MCBI-TMI. Alkylation by (+)-**17** and (+)-CBI-TMI were compared at a concentration of 10^{-5} M (25 °C, 24 h) and the IOD% versus time data was normalized to previous data that compared (+)-MCBI-TMI, (+)-CCBI-TMI, and (+)-CBI-TMI.

Table 2. Cytotoxic Activity[a]

agent	IC_{50} (L1210), μM	agent	IC_{50} (L1210), μM
	Natural Enantiomers		
(+)-**13**	11	(+)-CBI	nd
(+)-**12**	0.07	(+)-*N*-BOC-CBI	0.08
(+)-**17**	2.0×10^{-5}	(+)-CBI-TMI	3.2×10^{-5}
	Unnatural Enantiomers		
(−)-**13**	13	(−)-CBI	11
(−)-**12**	0.3	(−)-*N*-BOC-CBI	0.9
(−)-**17**	1.7×10^{-3}	(−)-CBI-TMI	2.0×10^{-3}

[a] IC_{50} values ±10%, average of two or more assays run in triplicate.

DNA faster than (+)-CBI-TMI despite its intrinsic lower reactivity. Moreover, the comparable behavior of (+)-CCBI-TMI ≥ (+)-MCBI-TMI illustrates this effect is attributable simply to the presence of a C7 substituent independent of the substituent electronic effects.[7] We suggest this role is derived from the substituent contribution to the extended rigid length of the agent that leads to an increase in the inherent twist in the helical conformation of the DNA bound agent. The degree of twist in the linking N^2 amide induced upon binding contributes to the disruption of the vinylogous amide conjugation and an increase in the inherent reactivity of the agent, contributing to the catalysis of the DNA alkylation reaction.[9−18]

In Vitro Cytotoxic Activity. The results of a study of the cytotoxic properties of the C5-CO_2Me-CBI agents alongside the corresponding CBI agents are detailed in Table 2. Consistent with the enhanced stability of the C5-CO_2Me-CBI compounds, they displayed equivalent or slightly more potent cytotoxic activity than the corresponding CBI-based agents. Following trends established in prior studies, the natural enantiomers proved more potent than the unnatural enantiomers, and this effect was most pronounced with the TMI derivatives where the difference was 100-fold, mirroring the differences in the DNA alkylation efficiencies of the enantiomers. Analogous to prior studies, the *seco*-cyclopropane precursor **16** exhibited cytotoxic activity indistinguishable from the cyclopropane containing agent **17**.

5-Hydroxymethyl-CBI (23). In efforts to ensure that it was the electronic effects of the C5 methyl ester of **12**, **13**, and **17** that were responsible for the distinctions with the corresponding CBI-based analogues and not a steric

Scheme 5

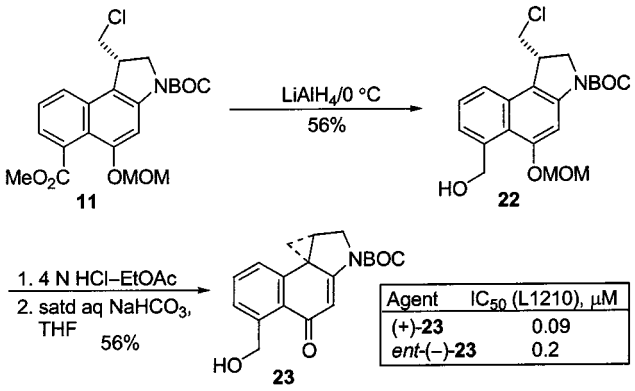

Table 3. Acid-Catalyzed Solvolysis Reactivity

	23	*N*-BOC-CBI	**12**
k, s^{-1} (pH 3.0)	1.62×10^{-6}	1.45×10^{-6}	0.81×10^{-6}
$t_{1/2}$, h (pH 3.0)	119	133	236
rel. stability	0.9×	1.0×	1.8×

effect derived from its proximal location to the C4 carbonyl, the two enantiomers of the 5-hydroxymethyl-CBI derivative **22** were prepared for comparative examination (Scheme 5). Reduction of the methyl ester of resolved **11** with $LiAlH_4$ (6 equiv, 0 °C, THF, 3 h) provided **22** (56%). Removal of the MOM ether of **22** (HCl, *i*-PrOH/THF) followed by treatment with saturated aqueous $NaHCO_3$ induced spirocyclization and afforded **23** (56%).

Consistent with expectations based on the electronic properties of the C5 substituent, the *N*-BOC derivative of 5-hydroxymethyl-CBI (**23**, $k = 1.62 \times 10^{-6}$ s^{-1}, $t_{1/2} =$ 119 h) was less stable than **12** ($t_{1/2} = 236$ h) and only slightly less stable (0.9×) than *N*-BOC-CBI ($t_{1/2} = 133$ h) to solvolysis at pH 3 (Table 3). This indicates that the distinctions in reactivity correlate well with expected electronic effects and are apparently unperturbed by potential steric effects related to the 4,5 substitution relationship. In addition, the two enantiomers of **23** exhibited a cytotoxic potency consistent with this relative level of stability (Scheme 5). This expected behavior of **23** relative to **12** and *N*-BOC-CBI suggest that the distinctions observed between **12** and *N*-BOC-CBI were due to the electronic, and not steric, effects of the C5 substituent.

Conclusions

A short and effective synthesis of *N*-BOC-C5-CO_2Me-CBI (**12**) and its immediate precursors is detailed. Its evaluation allowed a comparison of the electronic effects of C5 versus C7 substituents on the chemical and functional reactivity of the agents and the impact this may have on their biological properties. Solvolysis studies of *N*-BOC-C5-CO_2Me-CBI (**12**) and its comparison with related agents revealed that the introduction of C5 methyl ester slowed the rate of acid-catalyzed solvolysis (1.8×) without affecting the inherent reaction regioselectivity (>20:1). The comparison of the X-ray structure of the *N*-CO_2Me derivatives of C5-CO_2Me-CBI and CBI revealed beautiful correlations between the structures, the reaction regioselectivity, and the relative reactivity. The greater stability of **12** correlated exceptionally well with a shortened N2−C2a bond length (1.386 vs 1.390 Å) and smaller χ_1 dihedral angle (8.1° vs 21.2°) indicative of greater vinylogous amide conjugation and is accompanied by diminished cross-conjugated cyclopropane conjugation (shorter bond lengths). The DNA alkylation selectivities of the natural and unnatural enantiomers of **17** were unperturbed by the C5 methyl ester and identical to those of (+)- and (−)-CBI-TMI. The most significant distinction observed was the effect of C5 versus C7 substitution on the rate of DNA alkylation. As previously reported, C7 substituents (−CN and −OMe) were found to *increase* the rate of DNA alkylation independent of the substituent effect on intrinsic reactivity. By contrast, agents containing the C5-CO_2Me-CBI alkylation subunit displayed an expected *decrease* in the rate of DNA alkylation consistent with the substituent effect on intrinsic reactivity. These observations underscore the unique behavior of (+)-CCBI-TMI bearing a C7 cyano group, which was intrinsically more stable than (+)-CBI-TMI but was found to alkylate DNA at a faster rate. We attribute this latter behavior to the C7 cyano substituent role in increasing the rigid length of the alkylation subunit increasing the degree of DNA binding-induced twist, activating the cyclopropane ring toward nucleophilic attack, and contributing to DNA alkylation catalysis.

Although not central to our interests in examining **16** and **17**, their effective DNA alkylation properties and their comparable cytotoxic activities indicate that the C5 position is a viable position for alkylation subunit modification. Moreover, the C5 ester provides the opportunity for implementation of several approaches to enhancing therapeutic selectivity, including amide linkage to tumor targeted antibodies or cellular active transport substrates, as well as the preparation of lactone prodrugs.

Experimental Section

Methyl 8-Hydroxy-6-nitro-1-naphthoate (6). A suspension of **5** (50.0 mg, 233 μmol) in CH_3OH (5.8 mL) was treated with concentrated H_2SO_4 (26 μL, 465 μmol), and the mixture was warmed at reflux for 4 h. The reaction solution was cooled, diluted with H_2O (25 mL), and extracted with EtOAc (2 × 25 mL). The combined organic extracts were washed with H_2O (2 × 25 mL), dried (Na_2SO_4), and concentrated to afford **6** (56.8 mg, 100%) as an orange solid: mp 133−135 °C; ^{1}H NMR (acetone-d_6, 250 MHz) δ 10.44 (br s, 1H), 8.47 (d, $J = 2.3$ Hz, 1H), 8.28 (dd, $J = 3.2$, 6.0 Hz, 1H), 7.71 (m, 3H), 3.89 (s, 3H); ^{13}C NMR (acetone-d_6, 62.5 MHz) δ 170.9, 154.8, 147.1, 134.6, 132.8, 131.7, 131.6, 129.2, 128.3, 116.6, 103.6, 52.7; IR (film) ν_{max} 3299, 2953, 1699, 1511 cm^{-1}. Anal. Calcd for $C_{12}H_9NO_5$: C, 58.30; H, 3.67; N, 5.67. Found: C, 58.33; H, 3.76; N, 5.54.

***N*-(*tert*-Butyloxycarbonyl)-4-hydroxy-5-methoxycarbonyl-2-naphthylamine (7).** A solution of **6** (56.8 mg, 230 μmol) in THF (2.3 mL) was treated with 10% Pd/C (12 mg) and stirred under an atmosphere of H_2 for 2 h. At this point TLC analysis indicated that **6** was consumed. The reaction mixture was filtered through Celite and concentrated, and the residue was dissolved in THF (2.3 mL). The resulting solution was treated with BOC_2O (113 mg, 517 μmol), and the mixture was warmed at reflux under Ar for 9 h. The reaction solution was cooled and concentrated. Flash chromatography (SiO_2, 2 cm × 10 cm, 20% EtOAc/hexane) afforded **7** (63.1 mg, 87%) as pale yellow oil: ^{1}H NMR (acetone-d_6, 250 MHz) δ 9.63 (s, 1H), 8.57 (br s, 1H), 7.82 (m, 1H), 7.72 (d, $J = 1.8$ Hz, 1H), 7.41 (d, $J = 1.8$ Hz, 1H), 7.40 (s, 1H), 7.25 (d, $J = 1.9$ Hz, 1H), 3.87 (s, 3H), 1.49 (s, 9H); ^{13}C NMR (acetone-d_6, 62.5 MHz) δ 172.2, 153.9, 153.6, 139.4, 136.8, 130.6, 130.3, 126.2, 124.6, 118.2, 107.0, 104.7, 80.2, 52.6, 28.5; IR (film) ν_{max} 3328, 2969, 1705, 1546 cm^{-1}; HRMALDI−FTMS (DHB) *m*/*z* 340.1147 ($C_{19}H_{22}$-$BrNO_6 + Na^+$ requires 340.1155).

***N*-(*tert*-Butyloxycarbonyl)-5-methoxycarbonyl-4-(methoxymethoxy)-2-naphthylamine (8).** A solution of **7** (85 mg,

268 μmol) in CH_2Cl_2 (2.7 mL) was cooled to 0 °C, treated with *i*-Pr_2NEt (140 μL, 804 μmol) and MOMCl (41 μL, 536 μmol), and stirred at 25 °C for 12 h. The reaction mixture was concentrated. Flash chromatography (SiO_2, 2 cm × 10 cm, 20% EtOAc/hexane) afforded **8** (88 mg, 92%) as a white solid: mp 140−141 °C; ^{1}H NMR (acetone-d_6, 250 MHz) δ 8.66 (br s, 1H), 7.88 (d, *J* = 1.4 Hz, 1H), 7.82 (d, *J* = 8.3 Hz, 1H), 7.46 (apparent t, *J* = 7.3 Hz, 1H), 7.37 (d, *J* = 1.8 Hz, 1H), 7.26 (d, *J* = 6.4 Hz, 1H), 5.28 (s, 2H), 3.89 (s, 3H), 3.48 (s, 3H), 1.51 (s, 9H); ^{13}C NMR (acetone-d_6, 62.5 MHz) δ 171.8, 153.6, 153.3, 139.0, 136.2, 130.9, 129.4, 126.6, 123.6, 118.7, 108.4, 103.8, 95.7, 80.3, 56.6, 28.5; IR (film) ν_{max} 3342, 2920, 1722, 1628, 1544 cm^{-1}; HRMALDI−FTMS (DHB) *m*/*z* 384.1433 ($C_{19}H_{22}BrNO_6$ + Na^+ requires 384.1418). Anal. Calcd for $C_{19}H_{23}NO_6$: C, 63.15; H, 6.41; N, 3.88. Found: C, 63.12; H, 6.50; N, 3.86.

***N*-(*tert*-Butyloxycarbonyl)-1-bromo-5-methoxycarbonyl-4-(methoxymethoxy)-2-naphthylamine (9).** A solution of **8** (180 mg, 0.50 mmol) in THF (3.0 mL) was cooled to −78 °C and treated with TsOH·H_2O (9.5 mg, 50 μmol) in THF (0.5 mL) followed by NBS (107 mg, 0.60 mmol) in THF (1.5 mL). The reaction mixture was stirred for 1 h in the absence of light at −78 °C. The reaction solution was quenched with the addition of saturated aqueous $NaHCO_3$ (5 mL), diluted with H_2O (20 mL), extracted with EtOAc (3 × 30 mL), dried (Na_2SO_4), and concentrated. Flash chromatography (SiO_2, 2 cm × 10 cm, 5% EtOAc/hexane) afforded **9** (200 mg, 91%) as a yellow solid: mp 81−83 °C; ^{1}H NMR (acetone-d_6, 250 MHz) δ 8.25 (dd, *J* = 0.9, 8.7 Hz, 1H), 8.11 (s, 1H), 7.82 (br s, 1H), 7.66 (dd, *J* = 6.9, 8.3 Hz, 1H), 7.43 (dd, *J* = 0.9, 6.9 Hz, 1H), 5.36 (s, 2H), 3.92 (s, 3H), 3.50 (s, 3H), 1.53 (s, 9H); ^{13}C NMR (acetone-d_6, 62.5 MHz) δ 171.2, 153.1, 152.9, 136.9, 133.3, 131.6, 128.3, 124.9, 120.3, 104.9, 103.5, 95.9, 81.5, 56.9, 52.5, 28.3; IR (film) ν_{max} 3405, 2974, 1728, 1610 cm^{-1}; HRMALDI−FTMS (DHB) *m*/*z* 462.0535 ($C_{19}H_{22}BrNO_6$ + Na^+ requires 462.0523). Anal. Calcd for $C_{19}H_{22}BrNO_6$: C, 51.83; H, 5.04; N, 3.18. Found: C, 51.61; H, 5.36; N, 3.13.

2-[*N*-(*tert*-Butyloxycarbonyl)-*N*-(3-chloro-2-propen-1-yl)amino]-1-bromo-5-methoxycarbonyl-4-(methoxymethoxy)naphthalene (10). A solution of **9** (310 mg, 0.71 mmol) and Bu_4NI (13 mg, 35 μmol) in DMF (7.0 mL) was cooled to 0 °C and treated with NaH (60% dispersion in oil, 85.0 mg, 1.7 mmol). The reaction mixture was stirred at 0 °C for 30 min, treated with 1,3-dichloropropene (*E*/*Z* mixture of isomers) (196 μL, 2.1 mmol), and stirred at 25 °C for 9 h. The mixture was quenched with the addition of saturated aqueous NH_4Cl (3 mL) and extracted with EtOAc (3 × 30 mL). The combined organic extracts were washed with H_2O (5 × 30 mL), dried (Na_2SO_4), and concentrated. Flash chromatography (SiO_2, 3 cm × 10 cm, 20% EtOAc/hexane) afforded **10** as a mixture of rotamers and *E* and *Z* alkenes (330 mg, 91%) as a clear, colorless oil: ^{1}H NMR (acetone-d_6, 250 MHz) δ 8.40 (d, *J* = 8.7 Hz, 1H), 7.73 (apparent t, *J* = 6.9 Hz, 1H), 7.57 (d, *J* = 7.3 Hz, 1H), 7.21 and 7.16 (s, 1H), 6.19 (m, 2H), 5.37 (m, 2H), 4.42 (m, 1H), 4.03 (m, 1H), 3.94 (s, 3H), 3.50 (s, 3H), 1.54 and 1.32 (s, 9H); IR (film) ν_{max} 2974, 1733, 1703, 1610, 1590 cm^{-1}; HRMALDI−FTMS (DHB) *m*/*z* 536.0456 ($C_{22}H_{25}BrClNO_6$ + Na^+ requires 536.0446).

3-(*tert*-Butyloxycarbonyl)-1-(chloromethyl)-6-methoxycarbonyl-5-(methoxymethoxy)-1,2-dihydro-3*H*-benz[*e*]indole (11). A solution of **10** (26.8 mg, 52 μmol), AIBN (0.8 mg, 5.2 μmol), and Bu_3SnH (15.4 μL, 57.2 μmol) in benzene (0.52 mL) was degassed with Ar and warmed at 80 °C for 2 h under Ar. The reaction mixture was cooled to 25 °C and concentrated. Flash chromatography (SiO_2, 1.5 cm × 10 cm, 10% EtOAc/hexane) afforded **11** (21.4 mg, 95%) as a clear, colorless oil: ^{1}H NMR (acetone-d_6, 500 MHz) δ 7.93 (br s, 1H), 7.92 (d, *J* = 8.4 Hz, 1H), 7.54 (apparent t, *J* = 6.9 Hz, 1H), 7.27 (d, *J* = 7.0 Hz, 1H), 5.34 (s, 2H), 4.15 (m, 3H), 3.98 (dd, *J* = 2.9, 11.0 Hz, 1H), 3.91 (s, 3H), 3.73 (dd, *J* = 8.1, 11.0 Hz, 1H), 3.50 (s, 3H), 1.58 (s, 9H); ^{13}C NMR (acetone-d_6, 125 MHz) δ 171.3, 153.9, 152.3, 142.7, 131.8, 131.1, 126.9, 124.2, 122.8, 118.3, 116.7, 100.3, 95.5, 81.2, 56.3, 53.1, 52.0, 47.3, 41.2, 28.1; IR (film) ν_{max} 2954, 2913, 1733, 1698, 1615 cm^{-1}; HRMALDI−FTMS (DHB) *m*/*z* 458.1341 ($C_{22}H_{26}ClNO_6$ + Na^+ requires 458.1341).

Resolution of 11. The enantiomers of **11** were resolved on a HPLC semipreparative Diacel OD column (10 μm, 2 cm × 25 cm) using 2% *i*-PrOH/hexane eluant (14 mL/min, 90−100% recovery, 2.5 mg/injection). The enantiomers eluted with retention times of 46.3 min (unnatural enantiomer) and 39.5 min (natural enantiomer, α = 1.17). Natural (−)-(1*S*)-**11**: $[\alpha]^{23}_D$ −12 (*c* 0.03, THF). *ent*-(+)-(1*R*)-**11**: $[\alpha]^{23}_D$ +12 (*c* 0.03, THF).

***N*-(*tert*-Butyloxycarbonyl)-5-methoxycarbonyl-1,2,9,9a-tetrahydrocyclopropa[*c*]benz[*e*]indol-4-one (12).** A solution of **11** (4.8 mg, 11 μmol) in THF/*i*-PrOH (1:1, 367 μL) was treated with concentrated HCl (46 μL, 550 μmol) and stirred at 25 °C for 3 h. The reaction mixture was treated with saturated aqueous $NaHCO_3$ (500 μL) and stirred vigorously for 1 h. The resulting suspension was extracted with EtOAc (3 × 10 mL), and the organic extracts were combined, dried (Na_2SO_4), and concentrated. PTLC (SiO_2, 5 cm × 20 cm, 40% EtOAc/hexane) afforded **12** (1.7 mg, 44%, 56% based on conversion) as a clear, colorless film and recovered **11** (0.9 mg, 19%). For **12**: ^{1}H NMR (acetone-d_6, 400 MHz) δ 7.57 (apparent t, *J* = 7.6 Hz, 1H), 7.26 (dd, *J* = 1.0, 7.5 Hz, 1H), 7.19 (dd, *J* = 1.0, 7.9 Hz, 1H), 6.72 (br s, 1H), 4.06 (m, 2H), 3.82 (s, 3H), 3.09 (m, 1H), 1.71 (dd, *J* = 4.2, 7.8 Hz, 1H), 1.55 (t, *J* = 4.7 Hz, 1H), 1.53 (s, 9H); ^{13}C NMR (acetone-d_6, 100 MHz) δ 184.3, 171.4, 161.0, 152.2, 142.1, 135.2, 132.1, 130.7, 125.6, 123.9, 108.0, 102.8, 83.2, 53.8, 52.4, 35.4, 28.2, 24.8; IR (film) ν_{max} 3192, 2841, 1728, 1630, 1574 cm^{-1}; HRMALDI−FTMS (DHB) *m*/*z* 356.1483 ($C_{20}H_{21}NO_5$ + H^+ requires 356.1492). Natural (+)-**12**: $[\alpha]^{23}_D$ +64 (*c* 0.06, THF). *ent*-(−)-**12**: $[\alpha]^{23}_D$ −62 (*c* 0.05, THF).

5-Methoxycarbonyl-1,2,9,9a-tetrahydrocyclopropa[*c*]benz[*e*]indol-4-one (13). A solution of **11** (9.9 mg, 22.7 μmol) in 4 N HCl/EtOAc (1.0 mL) was stirred at 25 °C for 45 min. The solvent was removed under a stream of N_2, and the residue was dried under vacuum. The residue was then treated with THF-saturated aqueous $NaHCO_3$ (1:1, 1.0 mL), and the solution was stirred vigorously for 2 h. The reaction mixture was extracted with EtOAc (3 × 10 mL), dried (Na_2SO_4), and concentrated. Flash chromatography (SiO_2, 1 cm × 10 cm, 0−30% THF/EtOAc) afforded **13** (4.1 mg, 71%) as an off-white film: ^{1}H NMR (acetone-d_6, 400 MHz) δ 7.46 (apparent t, *J* = 7.5 Hz, 1H), 7.16 (d, *J* = 7.5 Hz, 1H), 7.09 (d, *J* = 7.8 Hz, 1H), 6.78 (br s, 1H), 5.48 (s, 1H), 3.85 (dd, *J* = 6.0, 10.4 Hz, 1H), 3.78 (s, 3H), 3.66 (d, *J* = 10.6 Hz, 1H), 3.09 (m, 1H), 1.63 (dd, *J* = 3.8, 8.1 Hz, 1H), 1.35 (t, *J* = 4.2 Hz, 1H); ^{13}C NMR (acetone-d_6, 125 MHz) δ 181.9, 172.2, 170.3, 141.7, 135.3, 132.4, 130.9, 125.2, 123.5, 96.0, 52.2, 51.1, 50.9, 34.0, 27.0; IR (film) ν_{max} 3236, 2923, 1728, 1610, 1544 cm^{-1}; HRMALDI−FTMS (DHB) *m*/*z* 256.0966 ($C_{15}H_{13}NO_3$ + H^+ requires 256.0968). Natural (+)-**13**: $[\alpha]^{23}_D$ +43 (*c* 0.06, THF). *ent*-(−)-**13**: $[\alpha]^{23}_D$ −44 (*c* 0.05, THF).

3-(5,6,7-Trimethoxyindol-2-carbonyl)-1-(chloromethyl)-5-hydroxy-6-methoxycarbonyl-1,2-dihydro-3*H*-benz[*e*]indole (16). A solution of **11** (2.6 mg, 6.0 μmol) in 4 N HCl/EtOAc (0.5 mL) was stirred at 25 °C for 1 h. The solvent was removed under a stream of N_2, and the residue was dried under vacuum. The residue was treated with 5,6,7-trimethoxyindole-2-carboxylic acid (**15**, 1.6 mg, 6.6 μmol), EDCI (3.4 mg, 18.0 μmol), and DMF (120 μL), and the resulting solution was stirred at 25 °C for 12 h. The solvent was removed under vacuum, and the residue was purified by PTLC (SiO_2, 10 cm × 20 cm, 5% THF/EtOAc) to afford **16** (2.3 mg, 74%) as a pale yellow film: ^{1}H NMR (acetone-d_6, 500 MHz) δ 10.28 (br s, 1H), 9.64 (br s, 1H), 8.08 (s, 1H), 7.98 (d, *J* = 8.5 Hz, 1H), 7.54 (apparent t, *J* = 7.0 Hz, 1H), 7.34 (d, *J* = 7.0 Hz, 1H), 7.14 (d, *J* = 2.2 Hz, 1H), 6.99 (s, 1H), 4.83−4.73 (m, 2H), 4.31−4.28 (m, 1H), 4.06 (m, 1H), 4.03 (s, 3H), 3.87−3.86 (m, 9H), 3.83−3.79 (m, 1H); IR (film) ν_{max} 3354, 2922, 2836, 1728, 1618 cm^{-1}; HRMALDI−FTMS (DHB) *m*/*z* 525.1443 ($C_{27}H_{25}ClN_2O_7$ + H^+ requires 525.1423). Natural (−)-(1*S*)-**16**: $[\alpha]^{23}_D$ −4.8 (*c* 0.06, THF). *ent*-(+)-(1*R*)-**16**: $[\alpha]^{23}_D$ +4.1 (*c* 0.05, THF).

***N*-(5,6,7-Trimethoxyindol-2-carbonyl)-5-methoxycarbonyl-1,2,9,9a-tetrahydrocyclopropa[*c*]benz[*e*]indol-4-one (17).** A solution of **16** (1.7 mg, 3.2 μmol) in CH_3CN (130 μL) was treated with DBU (1.0 μL, 6.5 μmol), and the mixture was stirred at 25 °C for 1 h. PTLC (SiO_2, 10 cm × 20 cm, 50%

THF/hexane) afforded **17** (1.2 mg, 76%) as a pale yellow film: ^{1}H NMR (acetone-d_6, 400 MHz) δ 10.51 (s, 1H), 7.61 (apparent t, J = 7.6 Hz, 1H), 7.29 (apparent t, J = 8.7 Hz, 2H), 7.15 (d, J = 2.2 Hz, 1H), 6.97 (s, 1H), 6.94 (s, 1H), 4.65 (dd, J = 5.0, 10.1 Hz, 1H), 4.53 (d, J = 10.1 Hz, 1H), 4.00 (s, 3H), 3.86 (s, 6H), 3.83 (s, 3H), 3.25 (m, 1H), 1.82 (dd, J = 4.4, 7.8 Hz, 1H), 1.75 (t, J = 4.7 Hz, 1H); IR (film) ν_{max} 3282, 2926, 1732, 1648 cm^{-1}; HRMALDI−FTMS (DHB) m/z 489.1667 ($C_{27}H_{24}N_2O_7$ + H$^+$ requires 489.165). Natural (+)-**17**: $[\alpha]^{23}_D$ +195 (c 0.02, THF). *ent*-(−)-**17**: $[\alpha]^{23}_D$ −184 (c 0.02, THF).

Solvolysis Regioselectivity: 3-(*tert*-Butyloxycarbonyl)-5-hydroxy-6-methoxycarbonyl-1-(methoxymethyl)-1,2-dihydro-3*H*-benz[*e*]indole (18). A solution of **12** (1.1 mg, 3.1 μmol) in CH_3OH (380 μL) containing 0.12 equiv of CF_3SO_3H was stirred at 0 °C for 72 h. $NaHCO_3$ (2.0 mg) was added, and the reaction mixture was stirred at 0 °C and warmed to 25 °C. The reaction mixture was diluted with H_2O (3 mL), extracted with EtOAc (3 × 5 mL), dried (Na_2SO_4), and concentrated. PTLC (SiO_2, 5 cm × 20 cm, 40% EtOAc/hexane) afforded **18** as a white film (0.9 mg, 75%, 92% based on conversion) and recovered **12** (0.2 mg, 16%). For **18**: ^{1}H NMR (acetone-d_6, 400 MHz) δ 7.86 (d, J = 8.4 Hz, 1H), 7.45 (dd, J = 7.0, 8.2 Hz, 1H), 7.24 (dd, J = 1.1, 7.0 Hz, 1H), 4.11−4.02 (m, 3H), 3.31 (s, 3H), 1.56 (s, 9H); IR (film) ν_{max} 3378, 2908, 2837, 1737 cm^{-1}; ESIMS m/z 388 (MH$^+$); HRMALDI−FTMS (DHB) m/z 288.1230 (MH$^+$ − BOC, requires 288.1230).

1-(Chloromethyl)-5-hydroxy-3-methoxycarbonyl-6-methoxycarbonyl-1,2-dihydro-3*H*-benz[*e*]indole (20). A solution of **11** (9.9 mg, 22.7 μmol) in 4 N HCl/EtOAc (1.0 mL) was stirred at 25 °C for 1 h. The solvent was removed under a stream of N_2, and the residue was dried under vacuum. The residue was dissolved in THF (0.50 mL) and treated with methyl chloroformate (5.3 μL, 68.1 μmol), $NaHCO_3$ (4.2 mg, 50 μmol), and the mixture was stirred at 25 °C for 2 h. The solution was diluted with EtOAc (10 mL) and poured into saturated aqueous NH_4Cl (10 mL). The layers were separated, and the aqueous layer was extracted with EtOAc (2 × 10 mL). The combined organic layers were dried (Na_2SO_4) and concentrated. Flash chromatography (SiO_2, 1 cm × 10 cm, 33% EtOAc/hexane) afforded **20** (5.8 mg, 59%) as a white solid: ^{1}H NMR (acetone-d_6, 400 MHz) δ 9.64 (s, 1H), 7.89 (d, J = 7.8 Hz, 1H), 7.76 (br s, 1H), 7.50 (dd, J = 7.0, 8.4 Hz, 1H), 7.28 (d, J = 6.6 Hz, 1H), 4.24−4.12 (m, 3H), 3.98 (dd, J = 3.1, 11.2 Hz, 1H), 3.85 (s, 3H), 3.81 (s, 3H), 3.70 (dd, J = 8.5, 11.2 Hz, 1H); IR (film) ν_{max} 3230, 2915, 2848, 1726, 1673 cm^{-1}; HRMALDI−FTMS (DHB) m/z 349.0729 ($C_{17}H_{16}ClNO_5$, M$^{+\bullet}$, requires 349.0717).

***N*-(Methoxycarbonyl)-5-methoxycarbonyl-1,2,9,9a-tetrahydrocyclopropa[*c*]benz[*e*]indol-4-one (21).** A solution of **20** (3.3 mg, 9.4 μmol) in CH_3CN (370 μL) was treated with DBU (2.8 μL, 18.9 μmol) and stirred at 25 °C for 1 h. PTLC (SiO_2, 10 cm × 20 cm, 66% THF/hexane) afforded **21** (2.9 mg, 100%) as a white solid: ^{1}H NMR (acetone-d_6, 400 MHz) δ 7.58 (apparent t, J = 7.6 Hz, 1H), 7.27 (d, J = 7.5 Hz, 1H), 7.20 (d, J = 7.9 Hz, 1H), 6.75 (br s, 1H), 4.12−4.09 (m, 2H), 3.82 (s, 3H), 3.81 (s, 3H), 3.13 (m, 1H), 1.74 (dd, J = 4.4, 7.9 Hz, 1H), 1.60 (t, J = 4.6 Hz, 1H); IR (film) ν_{max} 2915, 2847, 1726, 1630 cm^{-1}; HRMALDI−FTMS (DHB) m/z 314.1016 ($C_{17}H_{15}NO_5$ + H$^+$, requires 314.1023). Recrystallization from EtOAc/hexane provided white plates (mp 209−210 °C) suitable for X-ray structure determination.[31]

3-(*tert*-Butyloxycarbonyl)-1-(chloromethyl)-6-hydroxymethyl-5-(methoxymethoxy)-1,2-dihydro-3*H*-benz[*e*]indole (22). An ice-cooled solution of **11** (7.5 mg, 17 μmol) in THF (50 μL) was treated with $LiAlH_4$ (1 M in THF, 100 μL, 100 μmol) and stirred at 0 °C for 3 h. The reaction mixture was quenched with the addition of 0.1 N aqueous HCl (5 mL) and extracted with EtOAc (3 × 10 mL). The organic extracts were combined and washed with H_2O (2 × 20 mL), dried (Na_2SO_4), and concentrated. PTLC (SiO_2, 10 cm × 20 cm, 50% EtOAc/hexane) afforded **22** (3.9 mg, 56%) as a clear colorless film: ^{1}H NMR (acetone-d_6, 500 MHz) δ 7.68 (d, J = 8.1 Hz, 1H), 7.63 (d, J = 7.0 Hz, 1H), 7.47 (apparent t, J = 7.4 Hz, 1H), 5.43 (s, 2H), 5.25 (apparent t, J = 5.6 Hz, 2H), 4.23−4.08 (m, 4H), 3.67 (dd, J = 8.4, 11.0 Hz, 1H), 3.63 (s, 3H), 1.58 (s, 9H); IR (film) ν_{max} 3333, 2913, 2851, 1692, 1594 cm^{-1}; HRMALDI−FTMS (DHB) m/z 430.1399 ($C_{21}H_{26}ClNO_5$ + Na$^+$ requires 430.1392). Natural (−)-(1*S*)-**22**: $[\alpha]^{23}_D$ −3.5 (c 0.12, THF). *ent*-(+)-(1*R*)-**22**: $[\alpha]^{23}_D$ +4.0 (c 0.13, THF).

***N*-(*tert*-Butyloxycarbonyl)-5-hydroxymethyl-1,2,9,9a-tetrahydrocyclopropa[*c*]benz[*e*]indol-4-one (23).** A solution of **22** (1.1 mg, 2.7 μmol) in THF/*i*-PrOH (1:1, 90 μL) was treated with concentrated HCl (11 μL, 132 μmol) and stirred at 25 °C for 4 h. The reaction solution was treated with saturated aqueous $NaHCO_3$ (1.0 mL) and stirred vigorously for 1 h. The resulting suspension was extracted with EtOAc (3 × 10 mL), dried (Na_2SO_4), and concentrated. PTLC (SiO_2, 5 cm × 20 cm, 50% EtOAc/hexane) afforded **23** (0.5 mg, 56%) as a clear, colorless foam: ^{1}H NMR (acetone-d_6, 500 MHz) δ 7.49 (m, 2H), 7.02 (m, 1H), 6.74 (br s, 1H), 4.98 (dd, J = 5.5, 13.6 Hz, 1H), 4.78 (dd, J = 7.7, 13.9 Hz, 1H), 4.70 (dd, J = 5.9, 8.1 Hz, 1H), 4.04 (m, 2H), 3.04 (m, 1H), 1.66 (dd, J = 4.0, 7.7 Hz, 1H), 1.54 (s, 9H), 1.52 (t, J = 4.8 Hz, 1H); IR (film) ν_{max} 3360, 2919, 2849, 1728, 1621 cm^{-1}; HRMALDI−FTMS (DHB) m/z 328.1540 ($C_{19}H_{21}NO_4$ + H$^+$ requires 328.1543). Natural (+)-**23**: $[\alpha]^{23}_D$ +36 (c 0.03, THF). *ent*-(−)-**23**: $[\alpha]^{23}_D$ −35 (c 0.02, THF).

Aqueous Solvolysis Reactivity: pH 3. *N*-BOC-C5-CO_2Me-CBI (**12**, 50 μg) and *N*-BOC-C5-CH_2OH-CBI (**23**, 50 μg) were dissolved in CH_3OH (1.5 mL) and mixed with pH 3 aqueous buffer (1.5 mL). The buffer contained 4:1:20 (v:v:v) 0.1 M citric acid, 0.2 M Na_2HPO_4, and H_2O, respectively. The UV spectrum was measured at regular intervals every 2 h during the first day, every 12 h for another week, and every 24 h until no change was detected at the monitored absorption. For **12**, the decrease in the long-wavelength absorption at 313 nm and the increase in the short-wavelength absorption at 260 nm were monitored, Figure 3. The solvolysis rate constant (k = 0.81 × 10^{-6} s^{-1}) and half-life ($t_{1/2}$ = 236 h) were calculated from data recorded at the short-wavelength from the least-squares treatment (r = 0.998) of the slope of the plot versus $\ln[(A_f - A_i)/(A_f - A)]$. For **23**, the increase in the short-wavelength absorption at 260 nm was monitored providing k = 1.62 × 10^{-6} s^{-1} ($t_{1/2}$ = 119 h, r = 0.998) by the same treatment.

pH 2. A sample of **12** (50 μg) was dissolved in CH_3OH (1.5 mL) and mixed with pH 3 aqueous buffer (pH 2.0, 1.5 mL). The buffer contained 4:1:20 (v:v:v) 1.0 M citric acid, 0.2 M Na_2HPO_4, and H_2O, respectively. Immediately after mixing, the UV spectra of the solutions were measured against a reference solution containing CH_3OH (1.5 mL) and the aqueous buffer (1.5 mL), and these readings were used for the initial absorbance values. The solutions were stoppered, protected from light, and allowed to stand at 25 °C. UV spectra were recorded at regular intervals until constant values were obtained for the long-wavelength absorbances. The solvolysis rate constant was determined from the slope of the line obtained from linear least-squares treatment of the plot of $\ln[(A_f - A_i)/(A_f - A)]$ versus time using the long-wavelength measurements for **12**. The first-order rate constant determined under these conditions was k = 0.79 × 10^{-5} s^{-1} ($t_{1/2}$ = 24.7 h, r = 0.998).

DNA Alkylation Studies: Selectivity and Efficiency. The preparation of singly ^{32}P 5′ end-labeled double-stranded DNA, the agent binding studies, gel electrophoresis, and autoradiography were conducted according to procedures described in full detail elsewhere.[10] Eppendorf tubes containing the 5′ end-labeled DNA (9 μL) in TE buffer (10 mM Tris, 1 mM EDTA, pH 7.5) were treated with the agent in DMSO (1 μL at the specified concentration). The solution was mixed by vortexing and brief centrifugation and subsequently incubated at 25 °C for 24 h (natural enantiomers) and 25 °C (unnatural enantiomers) for 72 h. The covalently modified DNA was separated from the unbound agent by EtOH precipitation and resuspended in TE buffer (10 μL). The solution of DNA in an

(31) The author has deposited the atomic coordinates for **21** with the Cambridge Crystallographic Data Centre and has been allocated the deposition number CDCC 154560. The coordinates may be obtained upon request from the Director, Cambridge Crystallographic Data Centre, 12 Union Road, Cambridge, CB2 1EZ, U.K.

Eppendorf tube sealed with Parafilm was warmed at 100 °C for 30 min to induce cleavage at the alkylation sites, allowed to cool to 25 °C, and centrifuged. Formamide dye (0.03% xylene cyanol FF, 0.03% bromophenol blue, 8.7% Na_2EDTA 250 mM) was added (5 μL) to the supernatant. Prior to electrophoresis, the sample was denatured by warming at 100 °C for 5 min, placed in an ice bath, and centrifuged, and the supernatant (3 μL) was loaded directly onto the gel. Sanger dideoxynucleotide sequencing reactions were run as standards adjacent to the reaction samples. Polyacrylamide gel electrophoresis (PAGE) was run on an 8% sequencing gel under denaturing conditions (8 M urea) in TBE buffer (100 mM Tris, 100 mM boric acid, 0.2 mM Na_2EDTA) followed by autoradiography.

DNA Alkylation Studies: Relative Rates of Reaction. Following the procedure detailed above, Eppendorf tubes containing 5′ end-labeled w794 DNA (9 μL) in TE buffer (pH 7.5) were treated with (+)-**17** or (+)-CBI-TMI (1 μL, 10^{-5} M in DMSO). The solutions were mixed and incubated at 25 °C for 2, 4, 8, 12, and 24 h, respectively. Subsequent isolation of the alkylated DNA by EtOH precipitation, resuspension in TE buffer (10 μL, pH 7.5), thermolysis (30 min, 100 °C), PAGE, and autoradiography were conducted as detailed above. Relative rates for alkylation at the w794 high-affinity 5′-AATTA site were derived from the slopes of the plots of percent integrated optical density (IOD) of the high-affinity alkylation cleavage bands versus time (Figure 8).

Acknowledgment. We gratefully acknowledge the financial support of the National Institutes of Health (CA 41986), The Skaggs Institute for Chemical Biology, and Coulter Pharmaceuticals. We wish to thank Dr. Raj K. Chadha for the X-ray structure determination of **21**.

Supporting Information Available: ^{1}H NMR spectra of **5**, **7**, **10**−**13**, **16**−**18**, and **20**−**23**. This material is available free of charge via the Internet at http://pubs.acs.org.

JO001772G